JACC: CARDIOVASCULAR IMAGING
VOL. 8, NO. 2, 2015

ISSN 1936-878X/$36.00
PUBLISHED BY ELSEVIER INC.
http://dx.doi.org/10.1016/j.jcmg.2014.09.021

Combined IVUS and NIRS Detection of Fibroatheromas

Histopathological Validation in Human Coronary Arteries

Soo-Jin Kang, MD, PhD,*† Gary S. Mintz, MD,† Jun Pu, MD,*† Stephen T. Sum, PhD,‡ Sean P. Madden, PhD,‡ Allen P. Burke, MD,§‖ Ke Xu, PhD,† James A. Goldstein, MD,# Gregg W. Stone, MD,*† James E. Muller, MD,‡ Renu Virmani, MD,‖ Akiko Maehara, MD*†

ABSTRACT

OBJECTIVES This study assessed grayscale intravascular ultrasound (IVUS) and near-infrared spectroscopy (NIRS) detection of a histological fibroatheroma (FA).

BACKGROUND NIRS-detected, lipid-rich plaques (LRPs) and IVUS-detected attenuated plaques are considered to be vulnerable.

METHODS IVUS-attenuated plaque and NIRS-LRP (yellow or tan block chemogram) were compared with histopathology in 1,943 sections of 103 coronary arteries from 56 autopsied hearts.

RESULTS IVUS-superficial attenuation and NIRS-LRP showed a similar high specificity of approximately 95%, whereas IVUS-superficial attenuation alone had a poor sensitivity (vs. NIRS-LRP) in detecting FAs (36% vs. 47%; $p = 0.001$). Compared with FA sections with superficial attenuation, FA sections without superficial attenuation had a smaller plaque burden (57.1% vs. 67.7%), a larger arc of calcium (79.7° vs. 16.8°), and a lower prevalence of a ≥20% histological necrotic core (28% vs. 50%) or late FA (14% vs. 37%; all $p < 0.05$). Compared with FA sections with NIRS-LRP, FA sections without NIRS-LRP showed a smaller plaque burden (58.0% vs. 63.3%) and a lower prevalence of a ≥20% necrotic core (27% vs. 46%). Conversely, non-FAs with NIRS-LRP (vs. non-FAs without LRP) showed a larger plaque burden (55.1% vs. 46.3%), a greater prevalence of a ≥20% histological lipid pool (34% vs. 5%), and mostly pathological intimal thickening (50%) or fibrocalcific plaque (33%). When sections showed either IVUS attenuation or NIRS-LRP, the sensitivity for predicting a FA was significantly higher compared with IVUS attenuation alone (63% vs. 36%; $p < 0.001$) or NIRS-LRP alone (63% vs. 47%; $p < 0.001$). When sections showed both IVUS attenuation and NIRS-LRP, the positive predictive value improved compared with IVUS attenuation alone (84% vs. 66%; $p < 0.001$) or NIRS-LRP alone (84% vs. 65%; $p < 0.001$).

CONCLUSIONS NIRS-LRP was more accurate than IVUS for predicting plaque containing a necrotic core or a large lipid pool, and the combination was more accurate than either alone. (J Am Coll Cardiol Img 2015;8:184–94) © 2015 by the American College of Cardiology Foundation.

From the *Columbia University Medical Center, New York, New York; †Cardiovascular Research Foundation, New York, New York; ‡InfraReDx, Inc., Burlington, Massachusetts; §University of Maryland Medical Center, Baltimore, Maryland; ‖CVPath Institute, Gaithersburg, Maryland; and the #Division of Cardiology, William Beaumont Hospital, Royal Oak, Michigan. Dr. Mintz has received consulting fees from Boston Scientific, InfraReDx, Acist, and Volcano Corporation; and research grant support from Volcano Corporation. Dr. Pu has received research grants from Boston Scientific China. Drs. Sum, Madden, and Muller are current employees of InfraReDx. Dr. Burke was a consultant to InfraReDx for histological studies. Dr. Goldstein is an InfraReDx consultant and equity owner. Dr. Stone is a consultant to Boston Scientific, Volcano Corporation, and InfraReDx. Dr. Virmani has been a consultant to Abbott Vascular, Atrium, Biosensors International, Biotronick, Boston Scientific, Celonova, Cordis J&J, GlaxoSmithKline, Kona Medical, Lutonix, Medtronic, Merck Speakers Bureau, MicroPort Medical, Mitralign, OrbusNeich Medical, ReCor Medical, SINO Medical, Terumo, 480 Biomedical, and WL Gore. Dr. Maehara is a consultant to Boston Scientific and Acist; and has received research/grant support from Boston Scientific and speaker fees from St. Jude Medical and Volcano Corporation. All other authors have no relationships relevant to the contents of this paper to disclose. Morton Kern, MD, served as Guest Editor for this paper.

Manuscript received May 7, 2014; revised manuscript received September 5, 2014, accepted September 8, 2014.

Autopsy studies have demonstrated that sudden cardiac death and myocardial infarction are mostly caused by rupture of a preexisting necrotic core and/or lipid core-rich fibroatheroma (FA) (1-4). Similarly, in patients who have undergone percutaneous coronary intervention, unstable plaques detected by in vivo intravascular imaging modalities, including intravascular ultrasound (IVUS)-attenuated plaques, were frequently associated with distal embolization and post-stenting cardiac enzyme elevation (5-8). Intracoronary near-infrared spectroscopy (NIRS) has been validated to identify lipidic plaque (9-14). Extensive lipid-rich plaque (LRP) detected by NIRS was not only typical of culprit lesions in ST-segment elevation myocardial infarction, but it also predicted a high risk of periprocedural myocardial infarction. Recently, IVUS and NIRS were combined in a single catheter so that the 2 modalities could be acquired simultaneously (14,15). The aims of this histopathological validation study were to: 1) determine the accuracy of the grayscale IVUS and/or NIRS detection of a histological FA; 2) to clarify determinants of a false positive and a false negative IVUS or NIRS study; and 3) to determine the incremental benefit of the use of combined NIRS and grayscale IVUS.

SEE PAGE 195

METHODS

SUBJECTS. Human coronary specimens were obtained over a 2-year period from 62 autopsied patients (10). As approved by the Institutional Review Board, hearts were acquired from the National Disease Research Interchange (Philadelphia, Pennsylvania) or the International Institute for the Advancement of Medicine (Edison, New Jersey), which also provided information regarding age, sex, medical history, and cause of death. The following terms were designated as a cardiac cause of death: "myocardial infarction," "cardiac arrest," and "other cardiac cause."

Hearts were received within 48 h after death, maintained on ice at 4°C, and imaged within 96 h after death. Major coronary arteries were harvested for examination following in situ angioscopic screening to exclude occluded segments that were impassable by IVUS or NIRS catheters. Side branches were ligated to prevent blood loss during perfusion, and adventitial fat was kept intact. Each arterial segment was mounted in a unique custom fixture with vertical guideposts at 2-mm intervals as reference points when comparing imaging with histological studies. Both ends of the segment were attached to luer connectors that allowed fluid flow and catheter entry. A varistaltic pump (Manostat, Barnant Company, Barrington, Illinois) supplied pulsatile flow at 60 cycles/min, and a flow rate of approximately 130 ml/min with pressure maintained the physiological levels (80 to 120 mm Hg).

Exclusion criteria were vessels in which IVUS and NIRS images and histological sections could not be precisely matched, minimum plaque, and poor image quality. After excluding 2-mm-long sections with maximal plaque thickness of <0.3 mm, a total of 1,943 2-mm long sections from 103 vessels from 56 autopsied hearts were included in the final analysis.

IVUS IMAGE ACQUISITION AND ANALYSIS. An Atlantis SR Pro 40-MHz catheter attached to an iLab system (both Boston Scientific, Fremont, California) was advanced over a 0.014-inch guidewire through the coronary artery that was mounted in the fixture. IVUS imaging was performed using motorized pullback at 0.5 mm/s to include proximal and distal luer connectors. Image data were archived onto a CD-ROM and sent to an independent IVUS core laboratory (Cardiovascular Research Foundation, New York, New York) for off-line analyses. Finally, every IVUS frame was matched to its comparable histopathological slice by using vessel shape, side branches, perivascular structures, and distances from the luer connectors.

Grayscale IVUS analyses were performed using validated planimetry software (echoPlaque, INDEC Medical Systems, Santa Clara, California). Qualitative and quantitative measurements were performed according to the criteria of the American College of Cardiology consensus statement on IVUS (16). Calcification was brighter than the reference adventitia with acoustic shadowing, with or without reverberations. The arc of calcium was measured; the interobserver variability was 4.1° ± 1.9°. Superficial attenuated plaque was ultrasonic attenuation of deeper arterial structures that began closer to the lumen than to the adventitia despite the absence of calcium (6,8,9). Plaques with deep attenuation (i.e., leading edge of attenuation closer to the adventitia than to the lumen) (8) were not classified as attenuated plaque in this study. The arc of attenuation was measured in degrees and included only the attenuated region without calcification; the interobserver variability of the arc of the attenuation measurement was 4.3° ± 2.1°. If there was >1 arc of attenuation in a given image slice, the arcs were added.

All grayscale IVUS determinations were based on the observations of 2 independent experienced reviewers (S.K. and A.M.) who were blinded to

ABBREVIATIONS AND ACRONYMS

FA = fibroatheroma
IQR = interquartile range
IVUS = intravascular ultrasound
LCBI = lipid core burden index
LRP = lipid-rich plaque
MLA = minimal lumen area
NIRS = near-infrared spectroscopy
PIT = pathological intimal thickening

other data. Interobserver and intraobserver variability yielded good concordance for the diagnosis of attenuated plaque ($\kappa = 0.93$ and $\kappa = 0.97$, respectively).

NIRS IMAGE ACQUISITION AND ANALYSIS. Using the same protocol for IVUS imaging, a 3.2-Fr InfraReDx (Burlington, Massachusetts) NIRS catheter was advanced into the distal coronary vessel. Automated mechanical pullback was performed at a speed of 0.5 mm/s and 240 rpm. Catheter imaging included the luer fittings so that the catheter position within the custom fixture could be precisely known and registered with histology and IVUS. Raw spectra were acquired at a rate of 40 Hz (1 spectrum every 25 ms).

Following the pullback, the probability of lipid core plaque was displayed as a "chemogram," which is a digital color-coded map of the location and intensity of lipid viewed from the luminal surface; the X-axis indicated the pullback position in millimeters (pixels every 0.1 mm), and the Y-axis indicated the circumferential position in degrees (pixels every 1°) as if the vessel had been split open along its longitudinal axis (10). The chemogram algorithm processed the spectroscopic information into a probability of lipid core plaque and mapped it to a 128 (7-bit) red-to-yellow color scale, with the lowest probability of lipid shown as red and the highest probability shown as yellow. Yellow pixels (pixels above the threshold for the detection of lipidic plaque) were divided by all viable pixels in the chemogram to generate the lipid core burden index (LCBI) per mille (‰). The NIRS "block chemogram" is a summary metric that displayed the top 10th percentile probability for all measurements of the corresponding 2-mm-long chemogram section binned to 4 discreet colors: red ($p < 0.57$), orange ($0.57 \leq p < 0.84$), tan ($0.84 \leq p < 0.98$), and yellow ($0.98 \leq p$). The presence of a yellow or tan block defined LRP. NIRS image analyses were performed off-line using an in-house, Matlab-based software programmed at the Cardiovascular Research Foundation.

HISTOPATHOLOGY ANALYSIS AND DEFINITIONS. After the IVUS and NIRS images were obtained, segments were pressure-fixed in formalin and decalcified with ethylenediaminetetraacetic acid and sectioned into 2-mm-long blocks using the fixture's guideposts to correspond to the 2-mm-long IVUS and NIRS sections. Preparation of thin sections, staining, and histological analysis were performed at the CVPath Institute (Gaithersburg, Maryland). Histopathology slides of 5-μm thickness were prepared from the distal side of each 2-mm-long block and stained with hematoxylin-eosin and Russell-Movat's pentachrome as previously described (10). With Movat's pentachrome, elastic fibers stain black, collagen fibers stain yellow, proteoglycan stains green, and smooth muscle cells stain red. Histological features of the arteries were classified using a modified American Heart Association plaque classification method based on the agreement of 2 CVPath Institute pathologists (A.P.B. and R.V.) who were blinded to the IVUS and NIRS findings (3,4). Morphometric and/or quantitative assessment of the arc and size of the necrotic core, lipid pool, and calcification was determined by an automatic computer-assisted technique as previously described (10). The necrotic core and lipid pool were quantified as <10%, 10% to 20%, 20% to 40%, and >40% of the total plaque area. A histological FA included: 1) an early FA with an early necrotic core characterized by small cholesterol clefts and cellular debris with structured matrix; 2) a late FA with a late necrotic core characterized by increased cellular debris and cholesterol clefts, but with complete degradation of the extracellular structured matrix; and 3) a thin-cap FA with a large late necrotic core covered by a thin fibrous cap (<65 μm) (3,4,8). A focal FA was a FA that was confined within only 1 2-mm-long section. At least 2 non-FA sections separated individual FAs.

This database was collected for the development of the algorithm for infrared spectroscopy (10), and the sample size was based on this purpose. Gardner et al. (10) used 86 human coronary artery segments from 33 hearts and then tested 126 coronary segments from 51 hearts in a prospective study. We used the same database after excluding some cases that had nonqualified IVUS images or normal segments (maximum intimal thickness <0.3 mm).

STATISTICAL ANALYSIS. Data analyses were performed using SPSS version 12.0 (IBM Corporation, Armonk, New York) or SAS version 9.1 (SAS Institute Inc., Cary, North Carolina). Categorical data were expressed as absolute values and percentages and compared using chi-square statistics or Fisher's exact test. Continuous data were reported as median (interquartile range [IQR]) and compared using nonparametric Mann-Whitney tests. For section-level data, a model with a generalized estimating equation approach was used to compensate for potential cluster effects of multiple sections in the same patient and presented as least-square means with 95% confidence intervals. Interobserver and intraobserver variability were assessed by κ statistical analysis that corrected for the chance of simple agreement and accounted for systematic observer bias; a $\kappa > 0.80$ indicated good agreement, and a κ between 0.61 and 0.80 indicated moderate agreement. The p values

were adjusted with the generalized estimating equation method for repeated measures. Inferential statistical tests were conducted at the significance level of 0.05.

RESULTS

BASELINE PATIENT AND LESION CHARACTERISTICS. Median patient age was 63.0 years (IQR: 50.3 to 77.8 years); and 37 of the patients (66%) were men. Twenty-five (45%) patients died from cardiac causes (12 cardiac arrests, 6 myocardial infarctions, and 7 deaths from other cardiac causes), and 19 (34%) patients died from a cerebrovascular accident. Hypertension, diabetes mellitus, and smoking were documented in 32 (57%), 17 (30%), and 27 (48%) patients, respectively.

A total of 1,943 2-mm-long histological sections were analyzed. Figure 1 shows IVUS plaque attenuation, NIRS-LCBI, and NIRS-block chemogram analysis according to the pre-specified histological classification.

PREDICTION OF FIBROATHEROMA BY SECTION-LEVEL IVUS ANALYSIS. Only 67 of 1,577 2-mm-long, non-FA-containing sections showed superficial grayscale IVUS attenuation (false positive: 4%), whereas 234 (64%) of 366 2-mm-long FA-containing sections had no superficial grayscale IVUS attenuation (false negative: 64%) (Table 1). Compared with FA-containing sections with superficial attenuation, FA-containing sections without superficial attenuation had a larger lumen, a smaller plaque burden, a larger arc of calcium on IVUS (Table 1), and a smaller necrotic core on histology (Figure 2). Moreover, histological FAs with superficial grayscale IVUS attenuation were more often classified as a late FA versus histological FAs without superficial attenuation (37% vs. 14%; $p < 0.001$). Of the 81 of 136 (60%) FA-containing segments with no superficial IVUS

FIGURE 1 IVUS and NIRS Findings According to Plaque Classification

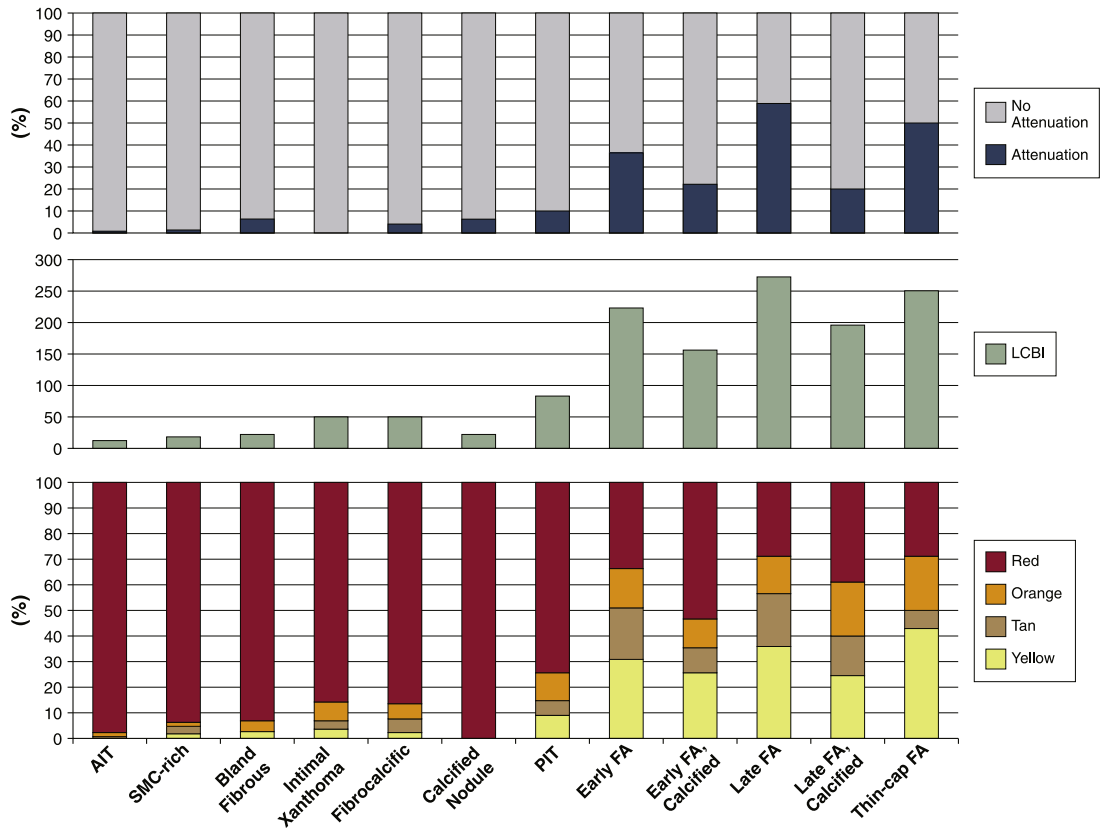

Frequency of IVUS attenuation **(top panel)**, lipid core burden index (LCBI) **(middle panel)**, and frequency of NIRS block chemogram **(bottom panel)**. AIT = adaptive intimal thickening; FA = fibroatheroma; IVUS = intravascular ultrasound; NIRS = near-infrared spectroscopy; PIT = pathological intimal thickening; SMC = smooth muscle cell.

attenuation, 46 (57%) were focal and confined within only 1 2-mm-long histological section. Finally, of the 677 sections with any amount of IVUS-detected calcification, 232 (34%) contained histological FAs.

Histological FAs with superficial attenuation (vs. histological FAs without superficial attenuation) were associated with smaller arcs of IVUS intraplaque calcium (16.8° [0° to 44.1°] vs. 79.7 [0° to 138.5°]; $p < 0.001$). In sections containing histological FAs, an arc of calcium cut-off value <35.5° separated attenuated from nonattenuated plaque (area under the curve: 0.70, 95% confidence interval [CI]: 0.642 to 0.748; $p < 0.001$). Similarly, histological FAs with superficial IVUS attenuation (vs. histological FAs without attenuation) were associated with greater plaque burden (67.7% [95% CI: 58.1% to 72.8%] vs. 57.1% [95% CI: 50.4% to 63.5%]; $p < 0.001$). A plaque burden of ≥62.3% separated attenuated from nonattenuated plaque (area under the curve: 0.72, 95% confidence interval: 0.663 to 0.775; $p < 0.001$).

PREDICTION OF FIBROATHEROMA BY SECTION-LEVEL NIRS ANALYSIS. As shown in Table 2, 193 of 366 FA-containing sections had no LRP (no yellow or tan NIRS block chemogram; false negative: 53%). Compared with FA-containing sections with NIRS-LRP, FA sections without NIRS-LRP were associated with a smaller IVUS plaque burden, less IVUS attenuation, and a lower prevalence of ≥20% histological necrotic core (27% vs. 46%) (Figure 2). However, there was no significant difference in the presence of calcium or arc of calcium between FA sections with versus without NIRS-LRP. In contrast, 92 of 1,577 non-FA-containing sections showed NIRS-LRP (false positive: 6%); this appeared to be related to a greater plaque burden and a larger external elastic membrane size on IVUS. In non-FA sections with LRP (yellow or tan NIRS block chemogram), the major histological lesion types were pathological intimal thickening (PIT) (50%) and fibrocalcific plaque (33%). A lipid pool ≥20% was observed in 34% of non-FA sections with NIRS-LRP, whereas only 5% of the non-FA

TABLE 1 Morphologic Characteristics Between Sections With Versus Without Intravascular Ultrasound Attenuation

	FA (n = 366)			Non-FA (n = 1,577)		
	Attenuation (n = 132)	No Attenuation (n = 234)	p Value	Attenuation (n = 67)	No Attenuation (n = 1,510)	p Value
Grayscale IVUS						
Lumen, mm^2	4.8 (3.3-7.0)	6.0 (4.5-7.5)	0.006	5.7 (3.9-7.3)	6.1 (4.4-8.2)	0.16
EEM, mm^2	14.8 (12.4-20.3)	14.3 (11.4-17.9)	0.29	14.9 (11.5-19.1)	11.5 (8.5-15.5)	0.009
P+M, mm^2	10.1 (7.6-13.4)	8.2 (6.1-10.7)	0.24	9.1 (7.2-12.0)	5.1 (3.2-8.0)	<0.001
Plaque burden, %	67.7 (58.1-72.8)	57.1 (50.4-63.5)	<0.001	61.4 (54.6-66.8)	46.4 (35.7-55.8)	<0.001
Arc of calcium, °	16.8 (0-44.1)	79.7 (0-138.5)	<0.001	0 (0-35)	0 (0-20.5)	0.010
Calcium	71 (54%)	161 (69%)	0.010	32 (48%)	413 (27%)	0.46
NIRS-LCBI	259.3 (97.7-408.7)	144.3 (0-317.9)	0.010	29.2 (0-171.9)	0 (0-23.5)	<0.001
NIRS block chemogram						
Red	34 (29%)	101 (43%)		45 (67%)	1369 (91%)	
Orange	22 (17%)	36 (15%)	0.005	7 (10%)	65 (4%)	<0.001
Tan	24 (18%)	38 (16%)		6 (9%)	41 (3%)	
Yellow	52 (39%)	59 (25%)		9 (13%)	35 (2%)	
Plaque type						
AIT				7 (10%)	631 (42%)	
SMC rich				2 (3%)	109 (7%)	
Bland fibrous				7 (10%)	94 (6%)	0.001
Intimal xanthoma				0 (0%)	28 (2%)	
Fibrocalcific				17 (25%)	362 (24%)	
Calcified nodule				1 (2%)	14 (1%)	
PIT				33 (29%)	272 (18%)	
Early FA	45 (34%)	78 (33%)				
Early FA, calcified	14 (11%)	48 (21%)				
Late FA	49 (37%)	34 (14%)	<0.001			
Late FA, calcified	17 (13%)	67 (29%)				
Thin-cap FA	7 (5%)	7 (3%)				

Values are generalized estimating equation least-square mean (95% confidence intervals) or n (%). Nonparametric (Mann-Whitney) test.

AIT = adaptive intimal thickening; EEM = external elastic membrane; FA = fibroatheroma; IVUS = intravascular ultrasound; LCBI = lipid core burden index; NIRS = near-infrared spectroscopy; P+M = plaque plus media; PIT = pathological intimal thickening; SMC = smooth muscle cell.

FIGURE 2 Comparison of Necrotic Core and Lipid Pool

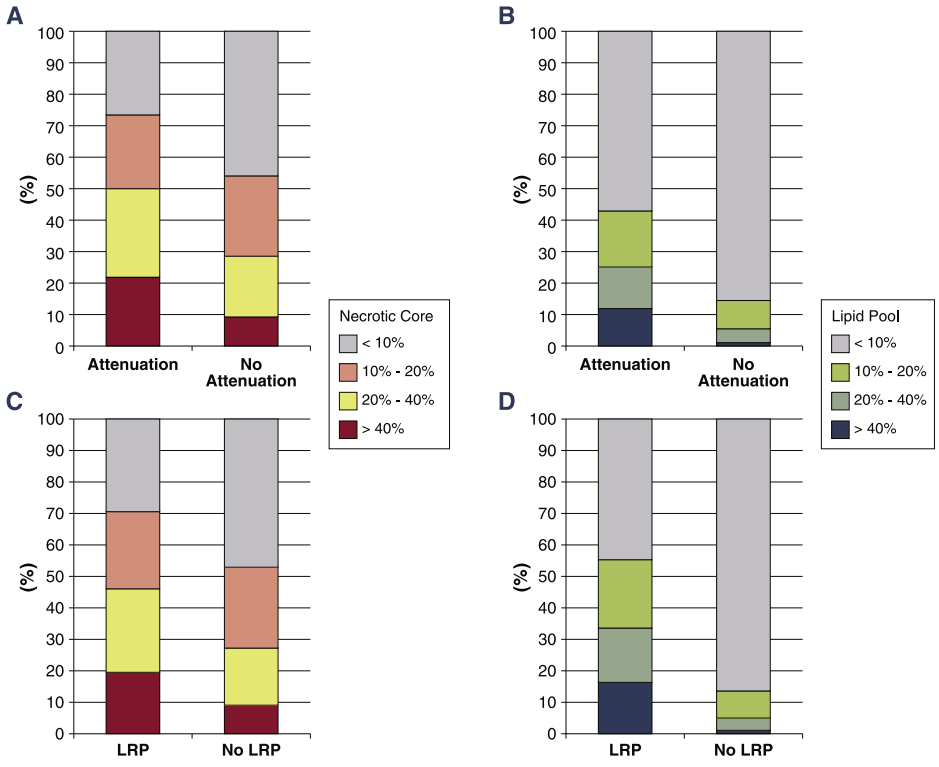

(A) Necrotic core between FA with versus without IVUS attenuation. **(B)** Lipid pool between non-FA with versus without IVUS attenuation. **(C)** Necrotic core between FA with versus without NIRS–lipid-rich plaque (LRP). **(D)** Lipid pool between non-FA with versus without NIRS-LRP. Abbreviations as in Figure 1.

sections without NIRS-LRP showed a lipid pool ≥20% (Figure 2). If, however, a yellow NIRS block chemogram was used to predict a histological FA, the sensitivity was 30%, the specificity was 97%, the positive predictive value was 71%, and the negative predictive value was 86%.

Overall, 61 of 136 FAs (45%) included no section with NIRS-LRP. Of these 61 FAs, 38 (62%) were focal and confined within only 1 2-mm-long histological section.

PREDICTION OF FIBERATHEROMA AT THE MINIMAL LUMEN AREA SITE. Overall, 103 histological sections from the minimal lumen area (MLA) site were interpreted to show 20 sections with adaptive intimal thickening, 5 sections with smooth muscle cell-rich plaque, 2 with bland fibrous plaque, 16 with fibrocalcific plaque, 16 with PIT, 16 with early FAs, 9 with calcified early FAs, 7 with late FAs, 9 with calcified late FAs, and 3 with thin-cap FAs. Table 3 compares grayscale IVUS and NIRS findings between 44 MLA sections with a FA versus 59 MLA sections without a FA.

In 44 MLA sections with a FA, 36 (82%) showed NIRS-LRP, whereas superficial attenuated plaque was seen in only 19 (43%). In the 25 FA-containing MLA sections without superficial plaque attenuation, 16 (64%) showed IVUS calcium with a median arc of 130.4° (IQR: 71.8° to 163.9°), and NIRS-LRP was observed in 20 sections (80%). Conversely, in 59 MLA sections without a FA, 58 (98%) had no attenuated plaque, and 56 (95%) showed no NIRS-LRP.

COMPARISON OF IVUS AND NIRS AND THE COMBINATION. Focal FAs were more frequently associated with both false negative NIRS-LRP (70% vs. 28%; $p < 0.001$) and false negative superficial IVUS attenuation (85% vs. 43%; $p < 0.001$) compared with FAs that spanned >1 histological section. Of the 232 FA-containing sections with IVUS-detectable calcium, 128 (55%) showed NIRS-LRP, whereas only 71 (30%) sections showed grayscale IVUS attenuation that was distinct from the shadowing caused by calcification. In the remaining 161 (70%) sections without attenuation, 65 (40%) had LRP on the NIRS block chemogram. Figure 3 demonstrates examples of a calcified lesion with NIRS-LRP.

TABLE 2 Morphologic Characteristics Between Sections With Versus Without NIRS-LRP

	FA (n = 366)			Non-FA (n = 1,577)		
	LRP (n = 173)	No LRP (n = 193)	p Value	LRP (n = 92)	No LRP (n = 1,485)	p Value
Grayscale IVUS						
Lumen, mm^2	5.1 (3.8–7.3)	6.0 (4.3–7.6)	0.47	6.2 (4.4–8.4)	6.0 (4.4–8.1)	0.23
EEM, mm^2	14.3 (11.9–18.0)	14.7 (11.5–18.5)	0.1	14.8 (9.8–18.3)	11.5 (8.5–15.4)	<0.001
P+M, mm^2	9.1 (7.1–11.7)	8.4 (6.2–1.1)	<0.001	7.8 (4.9–11.2)	5.1 (3.2–8.1)	<0.001
Plaque burden, %	63.3 (54.3–71.0)	58.0 (51.5–65.5)	<0.001	55.1 (49.9–61.4)	46.3 (35.4–56.2)	<0.001
Attenuation	76 (44%)	56 (29%)	0.003	15 (16%)	52 (3.5%)	<0.001
Arc of calcium, °	35.8 (0–107.9)	40.7 (0–117.9)	0.75	17.2 (0–130.0)	0 (0–20.3)	0.001
Calcium	128 (66%)	104 (60%)	0.44	48 (52.2%)	397 (26.7%)	<0.001
Plaque type						
AIT				6 (6.5%)	632 (42.5%)	
SMC rich				5 (5.4%)	106 (7.1%)	
Bland fibrous				3 (3.3%)	98 (6.6%)	
Intimal xanthoma				2 (2.2%)	26 (1.7%)	<0.001
Fibrocalcific				30 (32.6%)	349 (23.5%)	
Calcified nodule				0 (0%)	15 (1.0%)	
PIT				46 (50.0%)	259 (17.4%)	
Early FA	63 (36.4%)	60 (31.1%)				
Early FA, calcified	22 (12.7%)	40 (20.7%)				
Late FA	47 (27.2%)	36 (18.7%)	0.068			
Late FA, calcified	34 (19.7%)	50 (25.9%)				
Thin-cap FA	7 (4.0%)	7 (3.6%)				

Values are generalized estimating equation least-square mean (95% confidence interval) or n (%). Nonparametric (Mann-Whitney) test.
Abbreviations as in Table 1.

Accuracies of IVUS versus NIRS for the prediction of FA were compared at the MLA sites (Figure 4, left panel) and overall (Figure 4, middle panel). Table 4 summarizes factors affecting FA detection by IVUS or NIRS. For the prediction of a histological FA, smaller plaque burden, lesser amounts of necrotic core, and focal FA resulted in higher rates of false negatives by both IVUS and NIRS. Calcified plaques (that, by definition, were classified as "no attenuation") were also more likely to increase the rate of false negative IVUS assessment, whereas they rarely affected NIRS assessment. Histological PIT with a large lipid pool often had NIRS-LRP.

TABLE 3 Lesion Characteristics at the Minimal Lumen Area Site

	FA (n = 44)	Non-FA (n = 59)	p Value
Grayscale IVUS			
Lumen, mm^2	4.0 (3.5–4.4)	4.4 (3.9–4.8)	0.25
EEM, mm^2	13.5 (12.3–14.7)	10.0 (9.0–11.0)	<0.001
P+M, mm^2	9.4 (8.3–10.4)	5.7 (4.9–6.4)	<0.001
Plaque burden, %	57.8 (64.6–70.9)	56.4 (52.5–60.3)	<0.001
Attenuation	19 (43%)	1 (2%)	<0.001
Arc of attenuation, °	47.2 (24.9–70.5)	2.5 (-1.9–6.9)	<0.001
Arc of calcium, °	60.5 (38.4–82.6)	23.7 (9.9–37.6)	0.005
Calcium	26 (59%)	19 (31%)	0.02
NIRS-block chemogram			
LRP (tan or yellow)	36 (82%)	3 (5%)	<0.001
2 mm-LCBI	313.9 (262.6–365.2)	35.8 (12.2–59.5)	<0.001

Values are generalized estimating equation least square mean (95% confidence interval) or n (%). Nonparametric (Mann-Whitney) test.
Abbreviations as in Table 1.

Among the 136 FA-containing histopathologic segments, 34 (25%) showed both IVUS attenuation and NIRS-LRP, whereas 86 (63%) showed either IVUS attenuation or NIRS-LRP. Figure 4 (right panel) shows the accuracies of combining IVUS and NIRS assessment overall (Figure 4A) and at the MLA site (Figure 4B). When sections showed either IVUS-attenuation or NIRS-LRP, the sensitivity for predicting a FA was significantly higher compared with IVUS attenuation alone (63% vs. 36%; $p < 0.001$) or NIRS-LRP alone (63% vs. 47%; $p < 0.001$). When sections showed both IVUS attenuation and NIRS-LRP, the positive predictive value improved compared with IVUS attenuation alone (84% vs. 66%; $p < 0.001$) or NIRS-LRP alone (84% vs. 65%; $p < 0.001$). When either IVUS attenuation or NIRS-LRP was present at the MLA sites ($n = 103$), the sensitivity (89% vs. 43%; $p < 0.001$) and the negative predictive value (92% vs. 70%; $p < 0.001$) were much better than IVUS attenuation alone. However,

FIGURE 3 An Example of Calcified Plaque by Intravascular Ultrasound

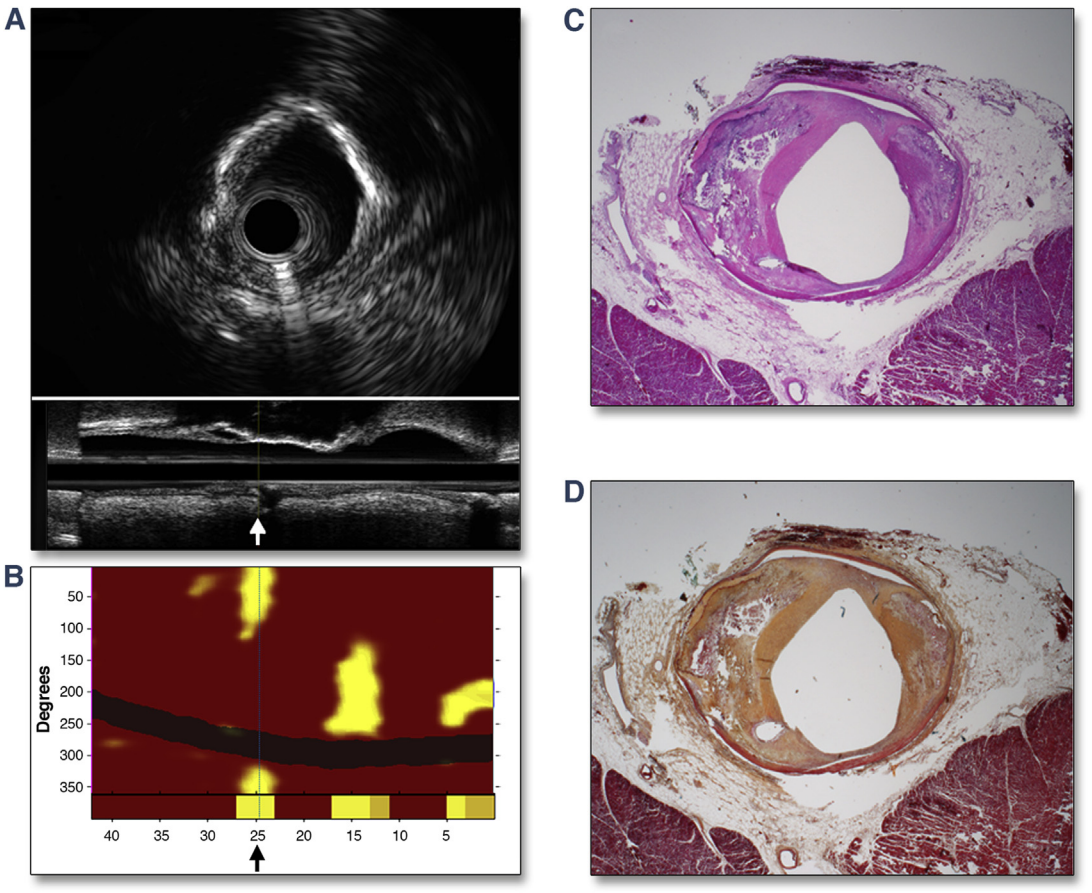

(A) Extensive superficial calcification. **(B)** At the corresponding site **(arrow)**, near-infrared spectroscopy chemogram showed "yellow" lipid-rich plaque. Histopathology slides demonstrated late fibroatheroma with calcified core. **(C)** Hematoxylin-eosin stain. **(D)** Russell-Movat pentachrome stain.

there were no significant differences compared with NIRS-LRP (all $p > 0.05$).

DISCUSSION

This study focused on the use of IVUS, NIRS, and/or the combination for identifying unstable plaques, specifically FAs. 1) Both IVUS attenuation and NIRS-LRP showed a high specificity of 96% and 94%, respectively, for predicting a histological FA. Conversely, superficial IVUS attenuation had a poor sensitivity of 36% that was explained by greater calcification (whose presence, by definition, precluded the "diagnosis" of attenuation), smaller plaque burden, and more focal and less advanced FA. 2) NIRS-LRP significantly improved the sensitivity for detecting a histological FA, especially in calcified lesions and lesions with a smaller plaque burden. 3) At the MLA site, the sensitivity, negative predictive value, and overall accuracy of NIRS were much better than that of IVUS. 4) When either IVUS attenuation or NIRS-LRP was present, the sensitivity for predicting FAs improved; when both IVUS-attenuation and NIRS-LRP were present, the positive predictive value also improved. However, this was less dramatic at MLA sites where the combination of IVUS and NIRS was superior to IVUS alone, but not to NIRS alone.

Attenuated plaque on grayscale IVUS indicates a high risk for no-reflow or an elevation in post-procedural creatine kinase-MB (5–7). Virtual histological IVUS and optical coherence tomography have shown attenuated plaque to be a marker for a large necrotic core and a thin-cap FA (5–7). Pu et al. (8) reported that histological FAs were found in 97%

FIGURE 4 Comparison of Accuracies of IVUS-Attenuated Versus NIRS-LRP

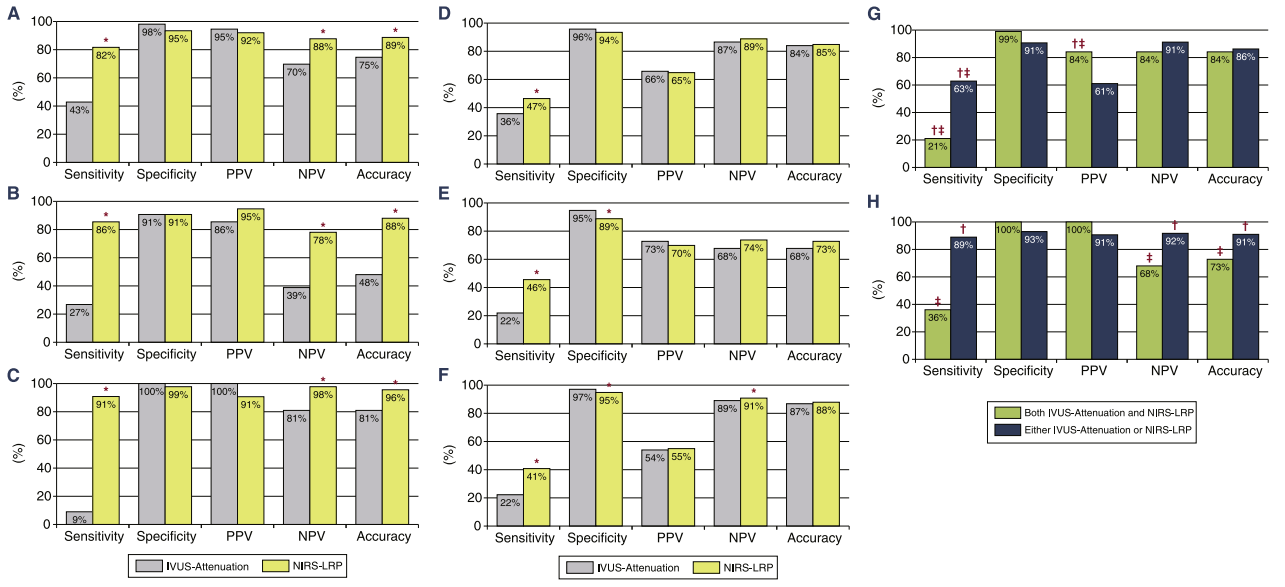

(A to C) Comparison of accuracies of IVUS attenuation versus NIRS-LRP at the minimum lumen area (MLA) sites. **(A)** In 103 sections at the MLA site (FA in 43%). **(B)** In 33 sections with IVUS-detected calcium ≥35.5° (FA in 67%). **(C)** In 52 sections with plaque burden <62.3% (FA in 21%). *p < 0.05 versus IVUS attenuation. **(D to F)** Comparison of accuracies of IVUS-attenuation versus NIRS-LRP. **(D)** The overall cohort of 1,943 sections (FA in 19%). **(E)** The cohort of 542 sections with IVUS-detected calcification ≥35.5° (FA in 37%). **(F)** The cohort of 1,578 sections with plaque burden <62.3% (FA in 13%). *p < 0.05 versus IVUS attenuation. **(G and H)** Accuracies of IVUS attenuation and/or NIRS-LRP for predicting FA in **(G)** all 1,943 sections or **(H)** in 103 sections at the MLA sites. **Green bars** indicate the presence of both IVUS attenuation and NIRS-LRP, whereas **blue bars** indicate the presence of either IVUS attenuation or NIRS-LRP. †p < 0.05 versus IVUS attenuation; ‡p < 0.05 versus NIRS-LRP. NPV = negative predictive value; PPV = positive predictive value; other abbreviations as in Figures 1 and 2.

of plaques with superficial IVUS attenuation, 31% of plaques with deep IVUS attenuation, and 27% of plaques without IVUS attenuation. Because the positive predictive value of deep attenuation was as poor as "no attenuation," the present analysis did not include deep attenuation and only reported superficial attenuation.

By definition, attenuated plaque excludes "attenuation (or, more correctly, shadowing) behind calcium." In the present study, 52% of plaques with IVUS-detected calcium were FAs. Although FAs were commonly associated with calcification, calcified lesions represented a major blind spot for IVUS. In the present analysis, the sensitivity of IVUS attenuation for detecting a histological FA was not >30% in both calcified lesions and lesions with a smaller plaque burden. When there is more calcium, diagnoses of FAs are less reliable by IVUS. In histological FAs, an arc of intraplaque calcium ≥35.5° and a plaque burden <62.3% best separated "no IVUS attenuation" from attenuation. Among FA-containing histological sections, 55% had an arc of calcium ≥35.5° and 57% a plaque burden <62.3%; thus, more than one-half of the FAs were at risk for being misdiagnosed. (However, when plaques with shadowing caused by calcification were added to the cohort of attenuated plaques in the absence of calcium, the sensitivity for prediction of an FA increased to 80%, but the specificity decreased to 69%, with a false positive rate of 30%.) Similar to previous data using NIRS and virtual histological IVUS (13), our study clearly demonstrated that calcium rarely affected the sensitivity of the NIRS block chemogram.

At MLA sites, NIRS-LRP showed significantly higher sensitivity (82% vs. 43%), negative predictive value (88% vs. 70%), and overall accuracy (89% vs.

TABLE 4 Factors Affecting Detection of a FA by IVUS or NIRS

IVUS Attenuation		NIRS-LRP	
False positive (non-FA with attenuation)	False negative (FA without attenuation)	False positive (non-FA with LRP)	False negative (FA without LRP)
Larger lipid pool	Calcification focal FA (≤2 mm) Larger lumen Smaller plaque burden Less necrotic core earlier stage of FA	PIT Fibrocalcific plaque Larger lipid pool Larger plaque burden	Focal FA (≤2 mm) Smaller plaque burden Less necrotic core

LRP = lipid-rich plaque; other abbreviations as in Table 1.

75%) versus IVUS attenuation. The benefit of NIRS assessment was remarkable, especially in MLA sections that contained more calcium and a smaller plaque burden. Although a smaller plaque burden was associated with false negative findings by both IVUS (FAs without attenuation) and NIRS (FAs without LRP), it was less likely to affect NIRS compared with IVUS. However, assessment of unstable lesion morphology cannot be confined to only the MLA site or the region with the largest plaque.

Although the NIRS block chemogram enhanced the sensitivity for FA detection relative to IVUS, it still had false positives or false negatives. First, histological FAs without NIRS-LRP (false negatives) were characterized by a smaller plaque burden with a lesser necrotic core, which suggested less advanced atherosclerotic disease. More importantly, 62% of histological FA segments without NIRS-LRP showed a focal FA. Conversely, the present data clearly demonstrated the high sensitivity (82%) and specificity (95%) of NIRS-LRP for detecting a histological FA at the MLA site where the atherosclerotic lesion looked the most significant. Second, non-FAs with NIRS-LRP (false positive) were mostly PIT (50%) with a large lipid pool. Because the NIRS signal is generated by lipid, such false positive results may indicate a stage of pathology preceding an FA. Moreover, 33% of non-FAs with NIRS-LRP were fibrocalcific plaques (plaques with a necrotic core completely surrounded by calcium that were classified as fibrocalcific), and NIRS may have been sensitive to the remnant necrotic core within the calcium. Despite no direct influence of calcium on the result of the NIRS block chemogram, a false positive NIRS-LRP was more likely associated with calcification, which may be partly explained by the high incidence of fibrocalcific plaque.

The findings demonstrate the complementary use of both sound (IVUS) and light (NIRS) to characterize plaques. IVUS is excellent for assessing structures and of calcification, whereas NIRS is a chemical method well-suited to the detection of lipid; the 2 are now available in a single catheter as the first combined intravascular imaging device. This present study demonstrated that combining IVUS and NIRS overcame some of the limitations of each technique and was more accurate than either IVUS or NIRS alone. For example, the use of superficial attenuation as the IVUS sign of an FA is frequently precluded by the presence of calcification; NIRS can detect lipid despite extensive calcification.

STUDY LIMITATIONS. Because this autopsy-based study evaluated hearts from 2 research tissue procurers, the results cannot be extended to the general population. Second, standard histological preparation requires dehydration of the tissue specimen before the tissue is embedded; this dissolves and elutes lipid, leaving an empty vacuole as presumptive evidence of previous lipid accumulation. Third, imaging was performed within 48 h post-mortem, and the specimen degradation tissue changes were not evaluated, which is a fundamental limitation of all autopsy studies. Fourth, despite our efforts to verify the correct matching among IVUS, NIRS, and histological sections, there might be inherent discordances that influenced accuracies. Because the purpose of this study was to determine the accuracy of the grayscale IVUS and/or NIRS detection of histological FAs, assessment of plaque rupture or thrombi was not considered in the present analysis. However, the impact of the present findings on clinical outcomes needs to be studied.

CONCLUSIONS

For the prediction of a plaque-containing necrotic core or large lipid pool, NIRS assessment improved the sensitivity and diagnostic accuracy compared with IVUS, especially in calcified plaque and lesions with small plaque burden. However, the combination of NIRS and IVUS, which is now possible in a single multimodality imaging catheter, was superior compared with NIRS or IVUS alone.

REPRINT REQUESTS AND CORRESPONDENCE: Dr. Akiko Maehara, Columbia University Medical Center, New York-Presbyterian Hospital, Cardiovascular Research Foundation, 111 East 59th Street, 12th Floor, New York, New York 10022. E-mail: amaehara@crf.org.

REFERENCES

1. Burke AP, Farb A, Malcom GT, Liang YH, Smialek J, Virmani R. Coronary risk factors and plaque morphology in men with coronary disease who died suddenly. N Engl J Med 1997;336:1276–82.

2. Farb A, Tang AL, Burke AP, Sessums L, Liang Y, Virmani R. Sudden coronary death: frequency of active coronary lesions, inactive coronary lesions, and myocardial infarction. Circulation 1995;92:1701–9.

3. Virmani R, Kolodgie FD, Burke AP, Farb A, Schwartz SM. Lessons from sudden coronary death: a comprehensive morphological classification scheme for atherosclerotic lesions. Arterioscler Thromb Vasc Biol 2000;20:1262–75.

4. Kolodgie FD, Burke AP, Farb A, et al. The thin-cap fibroatheroma: a type of vulnerable plaque: the major precursor lesion to acute coronary syndromes. Curr Opin Cardiol 2001;16:285–92.

5. Kubo T, Matsuo Y, Ino Y, et al. Optical coherence tomography analysis of attenuated plaques detected by intravascular ultrasound in patients

with acute coronary syndromes. Cardiol Res Pract 2011;2011:687515.

6. Wu X, Mintz GS, Xu K, et al. The relationship between attenuated plaque identified by intravascular ultrasound and no-reflow after stenting in acute myocardial infarction: the HORIZONS-AMI (Harmonizing Outcomes With Revascularization and Stents in Acute Myocardial Infarction) trial. J Am Coll Cardiol Intv 2011;4:495–502.

7. Jang JS, Jin HY, Seo JS, et al. Meta-analysis of plaque composition by intravascular ultrasound and its relation to distal embolization after percutaneous coronary intervention. Am J Cardiol 2013;111:968–72.

8. Pu J, Mintz GS, Biro B, et al. Insights into echo-attenuated plaques, echolucent plaques, and plaques with spotty calcification: novel findings from comparisons among intravascular ultrasound, near-infrared spectroscopy, and pathological histology in 2294 human coronary artery segments. J Am Coll Cardiol 2014;63:2220–33.

9. Pu J, Mintz GS, Brilakis ES, et al. In vivo characterization of coronary plaques: novel findings from comparing greyscale and virtual histology intravascular ultrasound and near-infrared spectroscopy. Eur Heart J 2012;33:372–83.

10. Gardner CM, Tan H, Hull EL, et al. Detection of lipid core coronary plaques in autopsy specimens with a novel catheter-based near-infrared spectroscopy system. J Am Coll Cardiol Img 2008;1:638–48.

11. Goldstein JA, Maini B, Dixon SR, et al. Detection of lipid-core plaques by intracoronary near-infrared spectroscopy identifies high risk of periprocedural myocardial infarction. Circ Cardiovasc Interv 2011;4:429–37.

12. Madder RD, Goldstein JA, Madden SP, et al. Detection by near-infrared spectroscopy of large lipid core plaques at culprit sites in patients with acute ST-segment elevation myocardial infarction. J Am Coll Cardiol Intv 2013;6:838–46.

13. Brugaletta S, Garcia-Garcia HM, Serruys PW, et al. NIRS and IVUS for characterization of atherosclerosis in patients undergoing coronary angiography. J Am Coll Cardiol Img 2011;4:647–55.

14. Madder RD, Steinberg DH, Anderson RD. Multimodality direct coronary imaging with combined near-infrared spectroscopy and intravascular ultrasound: initial US experience. Catheter Cardiovasc Interv 2013;81:551–7.

15. Wentzel JJ, van der Giessen AG, Garg S, et al. In vivo 3D distribution of lipid-core plaque in human coronary artery as assessed by fusion of near infrared spectroscopy-intravascular ultrasound and multislice computed tomography scan. Circ Cardiovasc Imaging 2010;3:e6–7.

16. Mintz GS, Nissen SE, Anderson WD, et al. American College of Cardiology Clinical Expert Consensus Document on Standards for Acquisition, Measurement and Reporting of Intravascular Ultrasound Studies (IVUS). A report of the American College of Cardiology Task Force on Clinical Expert Consensus Documents. J Am Coll Cardiol 2001;37:1478–92.

KEY WORDS fibroatheroma, imaging, intravascular ultrasound, near-infrared spectroscopy